http://dx.doi.org/10.5012/bkcs.2014.35.5.1375

Protein-Directed Synthesis of γ-Fe_2O_3 Nanoparticles and Their Magnetic Properties Investigation

Rouhollah Soleyman,[*] Ali Pourjavadi,[†,*] Nazila Masoud,[†] Akbar Varamesh, and Abolfazl Sattari[‡]

Polymer Science and Technology Division, Research Institute of Petroleum Industry (RIPI), P.O. Box 14115-143, Tehran, Iran. [*]E-mail: soleymanr@ripi.ir

[†]Polymer Research Laboratory, Department of Chemistry, Sharif University of Technology, Tehran, Iran [*]E-mail: purjavad@sharif.edu

[‡]Chemical Science and Technology Research Division, Research Institute of Petroleum Industry (RIPI), Tehran 1485733111, Iran

Received October 8, 2013, Accepted January 15, 2014

In this study, maghemite (γ-Fe_2O_3) nanoparticles were produced using gelatin protein as an effective mediator. Size, shape, surface morphology and magnetic properties of the prepared γ-Fe_2O_3 nanoparticles were characterized using XRD, FT-IR, TEM, SEM and VSM data. The effects of furnace temperature and time of heating together with the amount of gelatin on the produced gelatin-Fe_3O_4 nanocomposite were examined to prove the fundamental effect of gelatin; both as a capping agent in the nanoscale synthesis and as the director of the spinel γ-Fe_2O_3 synthesis among possible Fe_2O_3 crystalline structures.

Key Words : Nanostructures materials, Maghemite nanoparticles, Magnetic measurements

Introduction

In the last two decades, the use of magnetic nanoparticles in biomedical applications has had fast growth and during this explosive expansion, most interests in the clinical utilization of magnetic nanoparticles have focused on maghemite (γ-Fe_2O_3) nanoparticles because of their chemical inactivity, non-toxicity, biocompatibility, biodegradability, low particle dimension, large surface area and suitable magnetic properties.[1-4] Due to its spinel structure with two magnetically nonequivalent interpenetrating sub lattices, maghemite shows excellent magnetic behavior which has been used in magnetic resonance imaging (MRI) contrast enhancement,[5,6] bio-magnetic separations,[7] hyperthermia treatment,[8] and magnetic drug targeting.[9,10]

All these biomedical applications require nanoparticles with high magnetization values, sizes smaller than 100 nm, and narrow particle size distributions. Various methods have been reported for the synthesis of iron oxide nanoparticles *via* coprecipitation of Fe^{2+} and Fe^{3+} ions in alkaline medium,[11] using sonochemical synthesis,[12] microwave-hydrothermal,[13] and chemical solutions.[14] Moreover, some bio-scaffolds such as polysaccharide,[15] DNAs,[16] viruses,[17] proteins and peptides,[18-20] have been utilized in the synthesis of magnetic nanostructures.

In this study, we have prepared maghemite (γ-Fe_2O_3) nanoparticles after high temperature oxidation of gelatin-Fe_3O_4 nanocomposite, obtained from Fe^{3+} ions in alkaline medium in the presence of a protein (gelatin) as an effective capping agent. Overall, this method introduces a simple, soft and inexpensive procedure for synthesis of maghemite nanoparticles with narrow size distribution and pure crystalline phase. Also, the effect of temperature, time of heating and the amount of gelatin on the synthesis has been investigated by the use of various techniques.

Experimental

Materials. Pure gelatin, iron (III) sulfate and hydrazine hydrate solution ($N_2H_4 \cdot H_2O$, 80 wt %) were purchased from Merck Co. (Darmstadt, Germany) and Double distilled water was used for synthesis of nanoparticles.

Characterization. The powder particles were investigated by TEM (Modelno. CM120, Philips), XRD (D4 endeavor) (Cu Kα = 0.154 nm), and SEM (Modelno. S6100, Hitachi) for determining their shape, size and crystallinity. The interaction of nano-particles with protein, and their behavior before/after elimination of gelatin was investigated using an ABB Bomem MB-100 FT-IR spectrophotometer. The magnetic moment of the nanomaterials was measured using Lake Shore model 7400 vibrating sample magnetometer (VSM). X-ray photoelectron spectroscopy (XPS) graph was taken on a Thermo Electron Corporation spectrometer with an Al Kα (1486.6 eV) radiation.

Synthesis of γ-Fe_2O_3 Nanoparticles. The maghemite nanoparticles were obtained by hydrothermal treatment of $Fe_2(SO_4)_3$ solution in the presence of gelatin. Typically, aqueous $Fe_2(SO_4)_3$ solution (20 mL, 0.05 M) was stirred with different concentrations of gelatin solutions of same volumes (5 mL). After stirring for 5 min, 8 mL absolute ethanol was added to the above solution. Finally, 80 wt % hydrazine hydrate solution ($N_2H_4 \cdot H_2O$) (10 ml) was added drop wise with vigorous stirring. After 10 min stirring, the mixture was treated for 24 h at 100 °C, then protein was partially or completely eliminated at different furnace temperatures (400, 600 and 800 °C) and various times (0.5, 1 and 3 h).

Results and Discussion

In nature, it is shown that protein interactions not only direct nucleation of inorganic materials, but also control the crystal type, face, and size of these synthesized inorganic structures.[19] It has been reported that egg albumin protein could act as a unique mediator for the synthesis of Fe_3O_4 nanotubes. A mechanism for the construction of these nanotubes has been suggested by Geng *et al.*[20] Upon this proposed mechanism, we decide to challenge it with other proteins like gelatin. After many attempts and various changes in the reaction conditions for attaining corresponding nanotubes, no nano tubular structures were synthesized. Nonetheless, we could obtain γ-Fe_2O_3 nanoparticles instead, and we could prove synthesis of these nanoparticles and effect of gelatin protein in this synthesis. Actually, this discrimination can be correlated to the different conformations of different proteins, different orientation of proteins in the presence of ions, reaction conditions or perhaps existence of other ions and enzymes in the egg albumin in comparison to pure proteins.

A mechanism has been suggested for the synthesis of protein-mediated γ-Fe_2O_3 nanoparticles: Fe^{3+} ions and gelatin molecules start to self-assemble and form an organic-inorganic complex in the aqueous solution of ethanol. Then, these ions are reduced by hydrazine, and a gelatin-Fe_3O_4 nanocomposite structure is formed. In order to obtain detailed information about the surface composition, XPS analysis was employed, which is very sensitive to Fe^{2+} and Fe^{3+} cations and its related spectra are given in Figure 1. In the Fe2p high-resolution XPS spectrum (magnified region), the binding energies around 710 and 723 eV are related to Fe ($2p_{3/2}$) and Fe ($2p_{1/2}$), respectively, which are very close to the values of Fe_3O_4 published in the literature.[21,22] It is remarkable that no charge transfer satellite of Fe ($2p_{3/2}$) at about 720 eV is detected, indicating the formation of mixed oxides of Fe (II) and Fe (III), such as Fe_3O_4.[22]

By increasing the gelatin-Fe_3O_4 nanocomposite temperature, non-covalent bonds (hydrogen bonds) and covalent bands such as peptide bonds start rupturing; at 600 °C, gelatin completely is decomposed and perished, and spinel γ-Fe_2O_3 nanostructures are remained. The composition and phase purity of the prepared products were examined by XRD analysis (Figure 2). The XRD of the nanocomposite at 400 °C shows a noisy pattern. It is well-known that materials with incomplete crystallinity or blends of crystalline and amorphous phases can lead to noisy XRD and broad background intensity signals. Many polymers and semiconductors where crystallinity is constrained to a limited part of the molecular structure are examples of materials that can lead to XRD patterns with broad background fluctuations and noisy signals. Also, broad background XRD patterns can be obtained for nanosized material due to the dispersion effect induced by the distribution of small particle size.[23] Thermogravimetrical analysis shows that the major weight loss of gelatin occurred around 200-500 °C, and it can be one of the reasons of the noisy XRD pattern for the partially decomposed gelatin-Fe_3O_4 nanocomposite at 400 °C. Moreover, the XRD pattern of the nanoparticles at 600 °C has a good conformity with the spinel structure of γ-Fe_2O_3 nanoparticles (JCPDS card 39-1346) and its magnetic properties (Figure 3) suggest the γ-Fe_2O_3 synthesis as well. In addition, after increasing temperature up to 800 °C, the XRD pattern indicates that γ-Fe_2O_3 nanoparticles are completely converted to the pure rhombohedral because of good agreement of all XRD peaks with the XRD reference peaks of α-Fe_2O_3 (JCPDS card 33-0664). The loss of magnetic properties of product proves α-Fe_2O_3 nanoparticles formation as well.

The FT-IR spectra of gelatin-Fe_3O_4 nanocomposite (400 °C), γ-Fe_2O_3 nanoparticles (600 °C) and α-Fe_2O_3 nano-

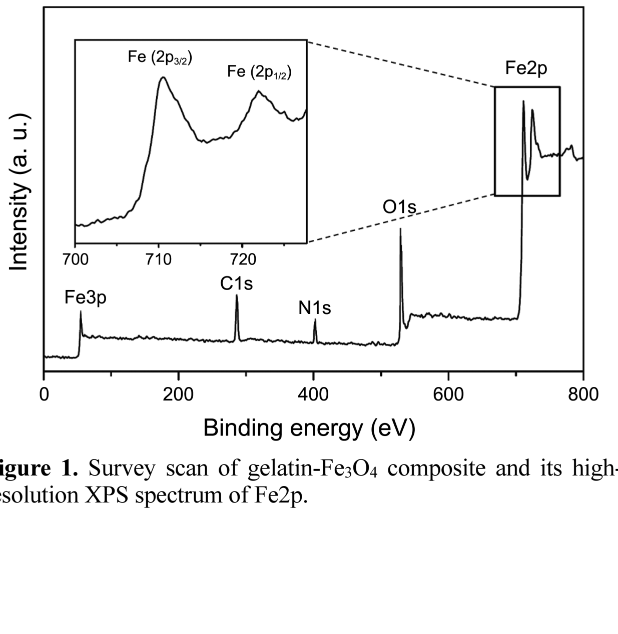

Figure 1. Survey scan of gelatin-Fe_3O_4 composite and its high-resolution XPS spectrum of Fe2p.

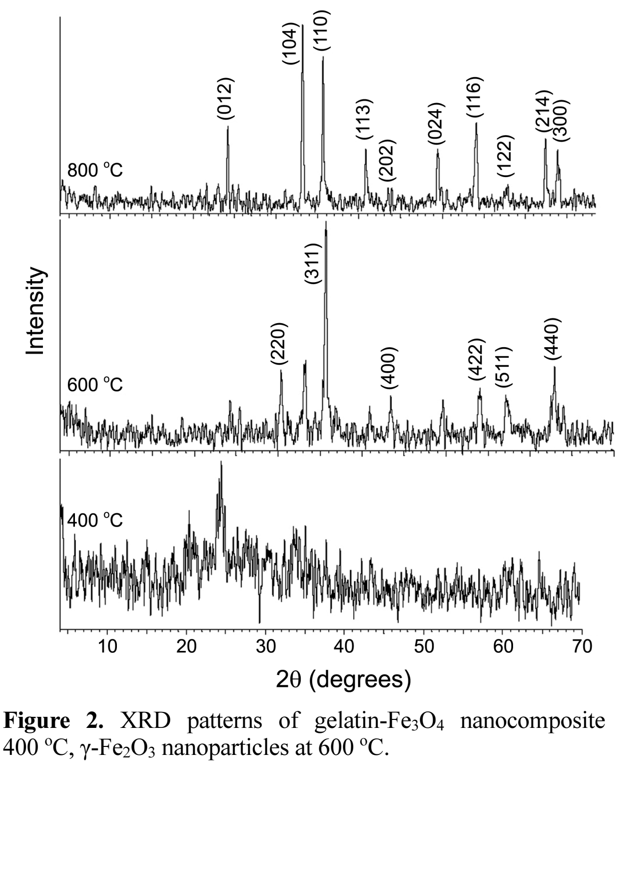

Figure 2. XRD patterns of gelatin-Fe_3O_4 nanocomposite at 400 °C, γ-Fe_2O_3 nanoparticles at 600 °C.

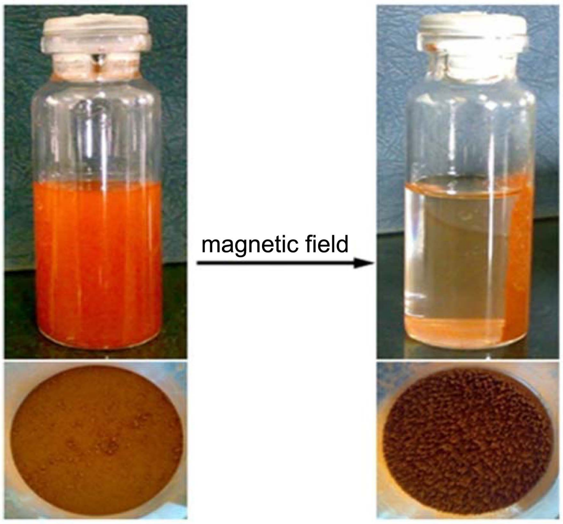

Figure 3. The produced maghemite nanoparticles dispersed in ethanol at absence and present of magnetic field.

particles (800 °C) are given in Figure 4. As the FT-IR peaks at 400 °C show, the gelatin protein in the gelatin-Fe_3O_4 nanocomposite has not been completely decomposed and the existence of gelatin residues in the Fe_3O_4 nanocomposite is perfectly obvious. The distinct peaks at 1623, 3140 and 3425 cm^{-1} indicate the existence of amide, hydroxyl and amine groups of gelatin at 400 °C, respectively. Obviously at 600 and 800 °C, the broad less intensive peaks around 3100-3400 cm^{-1} demonstrate the presence of hydroxyl groups on the surface of iron oxides.[23] The absorption peak at 588 cm^{-1} identifies the vibration of γ (Fe-O). Other peaks at pure maghemite include 444, 632, 1635, 3129 and 3398 cm^{-1}. At 800 °C, the peaks at 464 and 536 cm^{-1} are the characteristics of the α-Fe_2O_3 structure and the other peaks are similar to the γ-Fe_2O_3 structure.

Figure 5 indicates SEM images of samples before and after gelatin decomposition, 500 °C and 600 °C respectively. As shown, when protein has not been completely decomposed [Figure 5(a), 500 °C], γ-Fe_2O_3 nanoparticles are placed on the gelatin substrate; but after complete decomposition [Figure 5(b), 600 °C] only γ-Fe_2O_3 nanoparticles are found.

TEM images (Figure 6) were used to study the effect of gelatin on the formation of γ-Fe_2O_3 nanoparticles. Figure 6(a) shows that without the presence of gelatin in the reaction medium, the product has no distinct particles (because of agglomeration). Figure 6(b) shows the effect of 1.0 gram gelatin on the formation of γ-Fe_2O_3 nanoparticles, and proves that the nanoparticles have ellipsoid shape with mean particle size (about 70 nm). It has previously shown that proteins, such as gelatin, can play the role of capping agent in the synthesis of nanoparticles. In 2011, we have investigated on the role of gelatin in synthesis of silver nanoparticles.[24] Also; Lee *et al.*[25] have studied the effect of gelatin protein concentration on the synthesis of gold nanoparticles. Nonetheless; other data sets are more suggestive on effect of gelatin protein in nanoparticles synthesis. For instance, VSM data (Figure 7) verifies that the product synthesized without gelatin mediator, lacks great magnetization moment. Indeed, the obtained material is α-Fe_2O_3, not γ-Fe_2O_3 nanoparticles. Moreover, the related hysteresis loop (gelatin 1.0 g) at

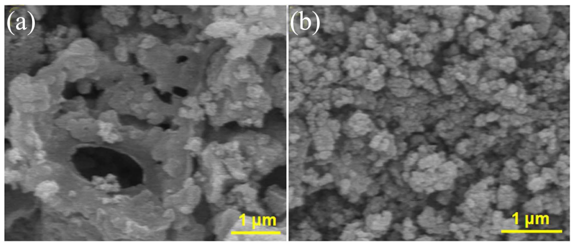

Figure 5. SEM images of (a) gelatin-Fe_3O_4 nanocomposite after 1 h curing at 500°C and (b) synthesized γ-Fe_2O_3 nanoparticles after 1 h curing at 600 °C (complete decomposition of gelatin).

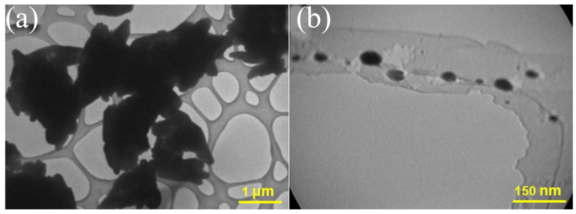

Figure 6. TEM images of synthesized materials (a) without any gelatin (b) using 1.0 g gelatin.

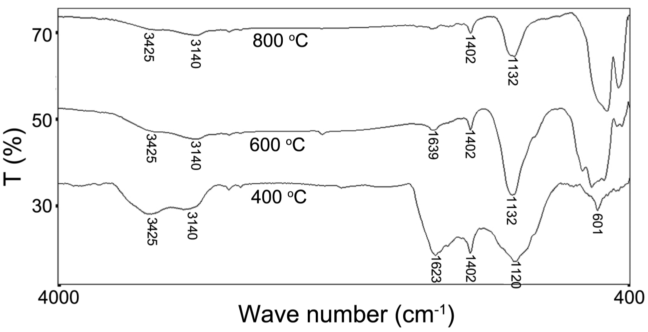

Figure 4. FT-IR spectra of gelatin-Fe_3O_4 nanocomposite at 400 °C, γ-Fe_2O_3 nanoparticles at 600 °C and α-Fe_2O_3 nanoparticles at 800 °C.

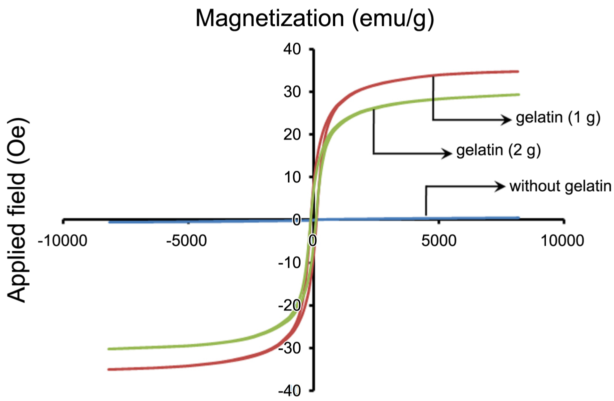

Figure 7. Effect of gelatin amounts on VSM hysteresis loop of synthesized materials.

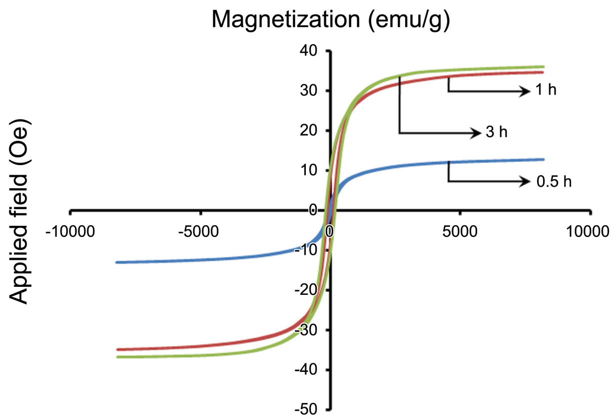

Figure 8. VSM curves of synthesized γ-Fe_2O_3 nanoparticles at 600 °C in different times of curing in furnace.

Figure 7 shows a great magnetization moment confirming magnetic properties of obtained γ-Fe_2O_3 nanoparticles. These data suggests a substantial effect of gelatin on nanoparticles behavior. The marvelous fact of our results is that heating the bulk Fe_3O_4 concludes in bulk α-Fe_2O_3, but heating the gelatin-Fe_3O_4 nanocomposites leads to γ-Fe_2O_3 nanoparticles. Briefly, these data confirm the role of gelatin protein as a good mediator and a key factor in the synthesis of γ-Fe_2O_3 nanoparticles.

Moreover, hysteresis diagrams (Figure 7, gelatin 2.0 g) show that increase in the amount of gelatin up to 2.0 gram doesn't considerably change the morphology and the magnetic properties of γ-Fe_2O_3 nanoparticles. Also, Figure 7 strictly confirms that the presence of gelatin is vital in the synthesis of γ-Fe_2O_3 nanoparticles in this procedure. Surprisingly, Figure 7 indicates that non-gelatin synthesized iron oxide nanoparticles (blue curve) don't have any magnetic properties.

In addition, the related VSM curves of the γ-Fe_2O_3 nanoparticles (Figure 8) demonstrate that time of heating in furnace has no distinguishable effect on magnetic properties of the nanoparticles after 1 h (Figure 8, 3 h) because of complete decomposition of the gelatin. However, the time of heating does have effect before 1 h (Figure 8, 0.5 h when the gelatin has not decomposed completely.

Conclusion

In summary, magnetic γ-Fe_2O_3 nanoparticles have been synthesized by a gelatin-assisted growth process without any organic toxic solvents. This approach provides a simple, novel, and feasible method for preparing stable-magnetic γ-Fe_2O_3 nanoparticles. Moreover, our study could prove effect of protein on size, shape and crystallinity of the synthesized inorganic nanoparticles.

References

1. Sun, C.; Lee, J. S.; Zhang, M. *Adv. Drug Deliv. Rev.* **2008**, *60*, 1252.
2. Laurent, S.; Forge, D.; Port, M.; Roch, A.; Robic, C.; Elst, L. V.; Muller, R. N. *Chem. Rev.* **2008**, *108*, 2064.
3. Mcbain, S. C.; Yiu, H. H.; Dobson, I. *Int. J. Nanomed.* **2008**, *3*, 169.
4. Veiseh, O.; Gunn, J. W.; Zhang, M. *Drug Deliv. Rev.* **2010**, *62*, 284.
5. Corot, C.; Robert, P.; Idée, J.; Port, M. *Adv. Drug Deliv. Rev.* **2006**, *58*, 1471.
6. Mccarthy, J. R.; Bhaumik, J.; Karver, M. R.; Erdem, S. S.; Weissleder, R. *Mol. Oncol.* **2010**, *4*, 511.
7. Shamim, N.; Hong, L.; Hidajat, K.; Uddin, M. S. *Separ. Sci. Technol.* **2007**, *53*, 164.
8. Villanueva, A.; Presa, P. D.; Alonso, J. M.; Rueda, T.; Mart, A.; Crespo, P.; Rivero, G. J. *J. Phys. Chem. C* **2010**, *114*, 1976.
9. Alexiou, C.; Diehl, D.; Henninger, P.; Iro, H.; Röckelein, R.; Schmidt, W.; Weber, H. *IEEE T. Appl. Supercon.* **2006**, *16*, 1527.
10. Kumar, A.; Jena, P. K.; Behera, S.; Lockey, R. F.; Mohapatra, S. *Nanomed. Nanotechnol.* **2010**, *6*, 64.
11. Lin, M. M.; Kim, D. K.; Haj, A. J.; Dobson, J. *IEEE T. Appl. Supercon.* **2008**, *7*, 298.
12. Shafi, K. V.; Ulman, A.; Yan, X.; Yang, N.; Estourne, C.; White, H.; Rafailovich, M. *Langmuir* **2001**, *17*, 5093.
13. Sreeja, V.; Joy, P. A. *Mater. Res. Bull.* **2007**, *42*, 1570.
14. Wu, Z. G.; Gao, J. F. *Micro. Nano. Lett.* **2012**, *7*, 533.
15. Wei, D.; Qian, W. *Colloid Surface B* **2008**, *62*, 136.
16. Wang, Z.; Zhang, J.; Ekman, J. M.; Kenis, P. J.; Lu, Y. *Nano Lett.* **2010**, *10*, 1886.
17. Balandin, A. A.; Fonoberov, V. A. *J. Biomed. Nano Technol.* **2005**, *1*, 90.
18. Dickerson, M. B.; Sandhage, K. H.; Naik, R. R. *Chem. Rev.* **2008**, *108*, 4935.
19. Wan, Y.; Zuo, G.; Liu, C.; Li, X.; He, F.; Ren, K.; Luo, H. *Polym. Adv. Tech.* **2010**, *22*, 2659.
20. Geng, B.; Zhan, F.; Jiang, H.; Guo, Y.; Xing, Z. *Chem. Commun.* **2008**, *44*, 5773.
21. He, H.; Gao, C. *ACS Appl. Mater. Interface* **2010**, *2*, 3201.
22. Morel, A. L.; Nikitenko, S. I.; Gionnet, K.; Wattiaux, A.; Lai-Kee-Him, J.; Labrugere, C; Chevalier, B; Deleris, G.; Petibois, C.; Brisson, A.; Simonoff, M. *ACS Nano* **2008**, *2*, 847.
23. Santolalla, C.; Alvarez-Ramirez, J.; Antonio de los Reyes-Heredia, J.; Chavez, J. *Ind. Eng. Chem. Res.* **2013**, DOI: 10.1021/ie303069y.
24. Pourjavadi, A.; Soleyman, R. *J. Nanopart. Res.* **2011**, *13*, 4647.
25. Neupane, M. P.; Lee, S. J.; Park, I. S.; Lee, M. H.; Bae, T. S.; Kuboki, K.; Uo, M.; Watari, F. *J. Nanopart. Res.* **2011**, *13*, 491.